As per UGC guidelines an electronic bar code is provided to secure your paper

International Journal for Modern Trends in Science and Technology
Volume 12, Issue 04, pages 706-717.
ISSN: 2455-3778 online
Available online at: http://www.ijmtst.com/vol12issue04.html
DOI: https://doi.org/10.5281/zenodo.19536644

ANN Based Decentralized Power Management for PV Wind Integrated Multi BESS EV Charging Infrastructure with State of Charge Balancing

Dr.Ch. Rambabu, Bh. Anusha, B. Karthik, G. Vishnu Vardhan Reddy, G. Vamsi

Department of Electrical and Electronics Engineering, Vasireddy Venkatadri Institute of Technology, Pedakakani, Namburu, Guntur, India.

To Cite this Article
Dr.Ch. Rambabu, Bh. Anusha, B. Karthik, G. Vishnu Vardhan Reddy & G. Vamsi (2026). ANN Based Decentralized Power Management for PV Wind Integrated Multi BESS EV Charging Infrastructure with State of Charge Balancing. International Journal for Modern Trends in Science and Technology, 12(04), 706-717. https://doi.org/10.5281/zenodo.19536644

Article Info
Received: 16 March 2026; Revised: 06 April 2026; Accepted: 10 April 2026.

Copyright © The Authors ; This is an open access article distributed under the Creative Commons Attribution License, which permits unrestricted use, distribution, and reproduction in any medium, provided the original work is properly cited.

KEYWORDS

Artificial Neural Network (ANN), Decentralized Power Management, Electric Vehicles (EVs), Battery Energy Storage System (BESS), State of Charge (SoC) Balancing, Hybrid Renewable Energy System.

ABSTRACT

The increasing penetration of electric vehicles (EVs) and renewable energy sources necessitates efficient and intelligent power management in decentralized energy systems. This paper presents an Artificial Neural Network (ANN)-based decentralized power management strategy for a hybrid photovoltaic (PV) and wind integrated multi-Battery Energy Storage System (BESS) supporting EV charging infrastructure. The proposed method enables real-time energy coordination among distributed sources and storage units without relying on centralized control, thereby improving system scalability and reliability. The ANN model predicts variations in renewable generation, load demand, and battery dynamics to optimize power distribution. A State of Charge (SoC) balancing mechanism is incorporated to ensure uniform energy utilization across multiple BESS units, preventing overcharging and deep discharging. This enhances battery lifespan and overall system efficiency. Simulation results indicate that the proposed approach achieves effective power sharing, improved stability, and faster response compared to conventional control methods. The framework demonstrates strong potential for smart grid applications with high renewable energy penetration and growing EV charging demands.

1. INTRODUCTION

The rapid electrification of transportation and the growing penetration of renewable energy sources have

significantly reshaped modern power systems. Electric vehicles (EVs) are increasingly being adopted worldwide due to their environmental benefits, high energy efficiency, and potential to reduce greenhouse gas emissions [1], [2]. However, the large-scale deployment of EV charging infrastructure introduces substantial challenges to the power grid, including increased peak demand, voltage instability, and load variability [3]. To mitigate these issues, integrating renewable energy sources such as photovoltaic (PV) and wind energy into EV charging stations has emerged as a promising solution for sustainable and eco-friendly energy supply [4], [5]. PV and wind energy systems are inherently intermittent and stochastic in nature, leading to fluctuations in power generation that can adversely affect grid stability and reliability [6]. To address these challenges, Battery Energy Storage Systems (BESS) are incorporated into hybrid renewable energy systems to store excess energy and supply power during periods of low generation [7]. In EV charging infrastructure, BESS plays a crucial role in peak shaving, load leveling, and enhancing the reliability of power delivery [8]. Particularly, the deployment of multiple distributed BESS units offers advantages such as improved redundancy, scalability, and localized energy management [9]. Despite these benefits, managing a multi-BESS system integrated with PV and wind sources in a dynamic EV charging environment is a complex task. Conventional centralized control strategies rely heavily on communication networks and centralized decision-making units, which may lead to increased latency, computational burden, and vulnerability to single-point failures [10]. These limitations have motivated the development of decentralized power management approaches, where individual components operate autonomously based on local measurements while contributing to overall system objectives [11]. Decentralized control frameworks offer enhanced flexibility, scalability, and robustness compared to centralized methods, making them suitable for modern smart grid applications [12]. In the context of EV charging infrastructure, decentralized strategies enable efficient coordination among distributed energy resources and storage units without requiring extensive communication infrastructure [13]. However, achieving optimal power sharing and coordination among multiple BESS units remains a significant challenge, particularly under varying load demands and renewable generation conditions [14]. One of the key aspects of efficient multi-BESS operation is maintaining balanced State of Charge (SoC) among storage units. Uneven SoC distribution can lead to overutilization of certain batteries, resulting in accelerated degradation, reduced lifespan, and inefficient system performance [15]. Therefore, SoC balancing techniques are essential to ensure uniform energy utilization, prevent overcharging and deep discharging, and enhance overall system reliability [16]. Existing approaches for SoC balancing include rule-based methods, droop control techniques, and optimization-based strategies; however, these methods often struggle to handle nonlinear system dynamics and uncertainties associated with renewable energy sources and EV charging behavior [17]. In recent years, Artificial Intelligence (AI) techniques have gained significant attention for addressing complex energy management problems in smart grids. Among these, Artificial Neural Networks (ANN) have demonstrated superior capability in modeling nonlinear relationships, forecasting energy generation and demand, and enabling adaptive control strategies [18]. ANN-based approaches have been successfully applied in PV power prediction, wind speed forecasting, load estimation, and battery management systems [19]. These capabilities make ANN a suitable candidate for developing intelligent power management systems in hybrid renewable energy-based EV charging infrastructure. Furthermore, ANN-based decentralized control frameworks provide the advantage of real-time decision-making and adaptability to changing system conditions without requiring centralized supervision [20]. By leveraging local data and predictive insights, ANN models can optimize power flow among PV, wind, BESS, and EV loads while ensuring system stability and efficiency. Integrating ANN with decentralized SoC balancing strategies can significantly enhance the performance of multi-BESS systems by enabling intelligent coordination and optimal energy distribution. Although several studies have investigated renewable-integrated EV charging systems and AI-based energy management techniques, limited work has focused on the combined implementation of ANN-based decentralized control with SoC balancing in multi-BESS environments. Addressing this research gap is essential for developing efficient, scalable, and reliable EV charging infrastructure capable of supporting future smart grid requirements.

Therefore, this paper proposes an ANN-based decentralized power management framework for PV–wind integrated multi-BESS EV charging infrastructure with SoC balancing. The proposed approach aims to achieve optimal power sharing, maintain balanced battery utilization, and enhance system reliability under dynamic operating conditions. The effectiveness of the proposed method is validated through simulation studies, demonstrating improved performance compared to conventional control strategies.

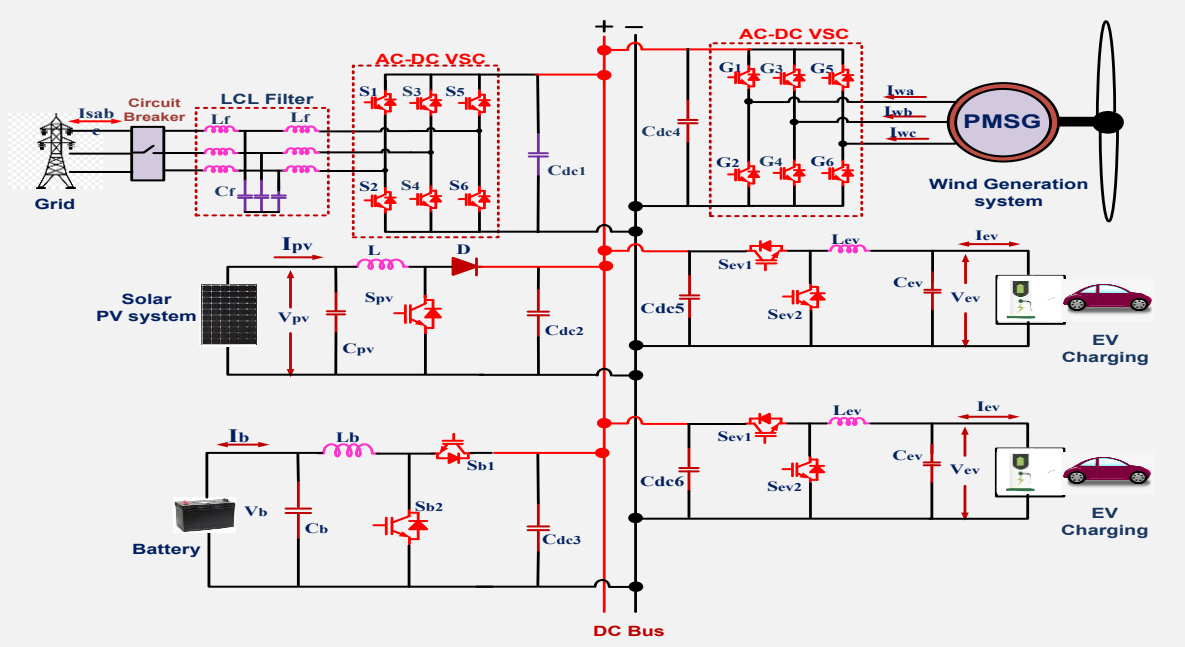

Fig. 1. Architecture of renewable based EVs charging station.

II. SYSTEM CONFIGURATION

The proposed system consists of a common DC-bus based hybrid EV charging architecture integrating the utility grid, solar PV system, wind generation system, and battery energy storage for coordinated power exchange. As shown in Fig. 1, the grid is connected to the DC bus through a circuit breaker, an LCL filter, and a three-phase AC–DC voltage source converter (VSC), enabling bidirectional power flow between the utility and the DC link. The solar PV source is interfaced to the DC bus through a boost DC–DC converter comprising an inductor, diode, switch, and input/output capacitors to regulate the PV power delivered to the DC link. The wind generation unit employs a permanent magnet synchronous generator (PMSG), whose three-phase output is converted to DC through an AC–DC VSC and then coupled to the common DC bus. A battery energy storage unit is also connected through a bidirectional buck–boost converter, allowing charging and discharging operation depending on renewable generation and EV demand. Two EV charging ports are supplied from the same DC bus through controlled DC–DC converter stages with inductive-capacitive filtering, which regulate the EV charging voltage and current. DC-link capacitors are placed at different interfacing points to maintain voltage stability and reduce ripple. Thus, the DC bus acts as the central power balancing node, where energy from PV, wind, grid, and battery sources is managed to satisfy EV charging demand under varying operating conditions.

III. MODELLING AND DECENTRALIZED POWER CONTROL OF MICRO SOURCES

The proposed system integrates multiple micro sources, including photovoltaic (PV) arrays, wind energy conversion systems (WECS), and Battery Energy Storage Systems (BESS), within a common DC bus architecture. Accurate modeling of these sources is essential for effective decentralized power control and reliable system operation under dynamic conditions.

A. Photovoltaic (PV) System Modeling

Photovoltaic (PV) systems are renewable energy technologies that convert sunlight directly into electrical energy using the photovoltaic effect. A single PV cell generates a small voltage, typically 0.5 to 0.6 V under standard test conditions (STC), and multiple cells are connected in series-parallel to form a PV module with sufficient voltage and current for power applications as

shown in Fig.2. The output characteristics of a PV panel are nonlinear and influenced by environmental conditions such as irradiance (G) and temperature (T). To extract the maximum power from a PV system under varying conditions, Maximum Power Point Tracking (MPPT) techniques are used. In modern electric vehicle (EV) charging stations and microgrid systems, photovoltaic (PV) solar energy is a widely used renewable source due to its sustainability and ease of integration. However, the voltage and power output of a solar PV panel are highly nonlinear and vary with environmental factors like irradiance and temperature. Therefore, a Maximum Power Point Tracking (MPPT) algorithm is essential for dynamically adjusting the operating point of the PV system to ensure maximum power extraction. After MPPT processing, a Buck converter is used to step down and regulate the output voltage to match the requirements of the DC load or battery charging system.

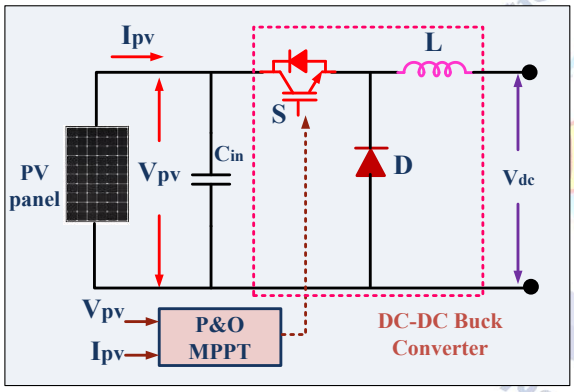

Fig. 2 solar PV P&O MPPT DC-DC Buck converter

1. PV Array Modeling

The output of a solar panel is modeled using the single-diode model, and its output current Ipv is expressed as:

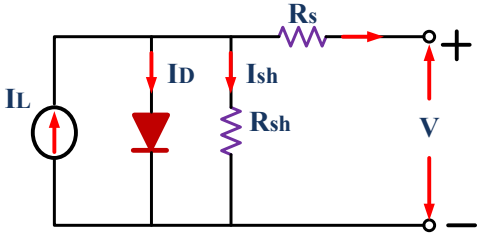

Fig. 3 equivalent model of PV solar.

$$I_{pv} = I_{Ph} - I_o\left(e^{\frac{q(V_{pv}+I_{pv}R_s)}{aKT}} - 1\right) - \frac{V_{pv}+I_{pv}R_s}{R_{sh}} \qquad (1)$$

Where:

- Iph is the photocurrent,
- I0 is the diode saturation current,
- Rs and Rsh are series and shunt resistances,
- a is the diode ideality factor,
- q is the electron charge,
- K is Boltzmann's constant,
- T is the cell temperature in Kelvin.

The photocurrent I_{ph} depends on the solar irradiance G and temperature:

$$I_{ph} = \left[I_{sc} + K_i\left(T - T_{ref}\right)\right] \cdot \frac{G}{G_{ref}} \qquad (2)$$

Where I_{sc} is the short-circuit current, and K_i is the temperature coefficient.

2. P&O MPPT Algorithm

The Perturb and Observe (P&O) algorithm works by periodically increasing or decreasing the operating voltage and observing the effect on the power output. The key idea is:

- If ΔP>0 and ΔV>0, increase voltage.
- If ΔP>0 and ΔV<0, decrease voltage.
- If ΔP<0, reverse the last change in voltage.

The current power is calculated as:

$$P(k) = V_{pv}(k) \cdot I_{pv}(k) \qquad (3)$$

And the previous power:

$$P(k-1) = V_{pv}(k-1) \cdot I_{pv}(k-1) \qquad (4)$$

The MPPT controller adjusts the duty cycle D of the Buck converter accordingly.

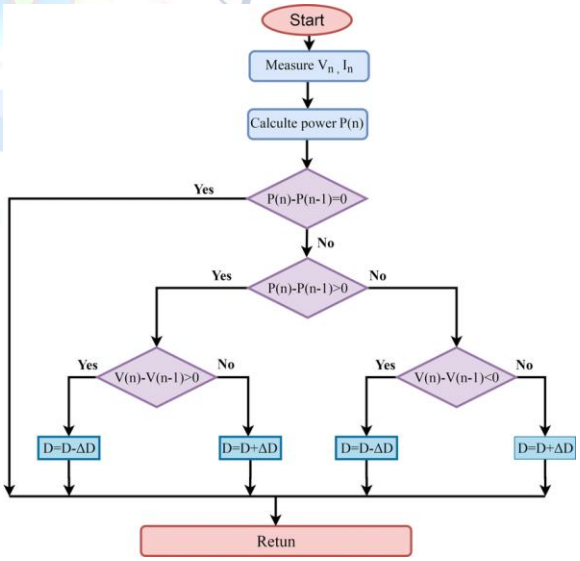

Fig.4 flow chart of P&O MPPT algorithm

B. Modeling and Designing of a Bidirectional Buck-Boost Converter

1. Introduction and System Overview

The combined strengths of lithium-ion batteries enable the development of efficient energy storage systems that leverage their high energy density and reliability, as shown in Fig. 5. The DC bus and these storage units can be effectively managed using a bidirectional buck–boost

converter. This converter facilitates power flow in both directions, allowing energy transfer from the DC bus to the battery during charging and from the battery to the load during discharging. Its capability to perform both step-down (buck) and step-up (boost) operations ensures proper voltage regulation under varying operating conditions. The converter plays a crucial role in maintaining stable DC bus voltage and controlling battery charging and discharging processes, thereby enhancing overall system performance and efficiency.

2. Operating Modes

The converter operates in two primary modes:

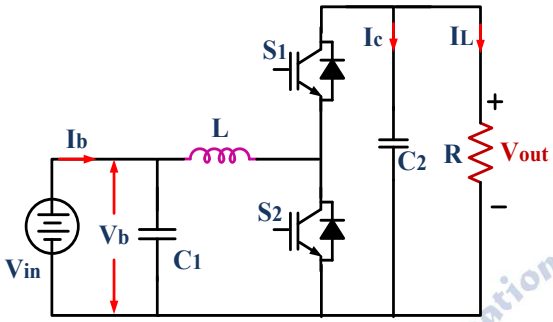

Fig.5 circuit diagram of DC-DC bidirectional buck boost converter

- **Buck Mode (Step-Down):** When the voltage on the DC bus is lower than the battery voltage (or supercapacitor voltage), the converter operates in buck mode to step down the voltage. This is typically used when discharging energy from the storage system to the bus or load.

- **Boost Mode (Step-Up):** When the voltage on the DC bus is higher than the storage voltage, the converter operates in boost mode to step up the voltage. This mode is used when charging the storage elements from the DC bus.

A single converter can operate in either mode by adjusting the duty cycle of its switching devices. In bidirectional operation, the power electronics (usually using MOSFETs or IGBTs) are arranged in an H-bridge or similar topology to allow current flow in both directions.

$$V_{out} = D \cdot V_{in} \quad (5)$$

Where: Vin is the input voltage (from the battery or DC bus), Vout is the regulated output voltage (to the load or storage device), D is the duty cycle, with 0<D<1.

3. Boost Mode (Step-Up Operation)

In boost mode, the converter increases the input voltage to a higher output voltage. The output voltage is expressed as:

$$V_{out} = \frac{V_{in}}{(1-D)} \quad (6)$$

Where: Vin is the lower voltage from the storage device or DC bus, Vout is the higher regulated voltage, D is the duty cycle, with 0<D<1.

4. Inductor and Capacitor Design

For both modes, an inductor L and output capacitor C are essential for smoothing the current and voltage ripples.

Inductor Design

To ensure continuous conduction mode (CCM) and limit the inductor current ripple (ΔIL), the inductor value can be estimated by:

$$L = \frac{(V_{in} - V_{out}) \cdot D}{f_s - \Delta I_L} \quad (7)$$

$$L = \frac{V_{in} \cdot D}{f_s - \Delta I_L} \quad (8)$$

Where: f_s is the switching frequency, ΔI_L is the desired peak-to-peak inductor current ripple.

Capacitor Design

The output capacitor C smooths the voltage ripple (ΔV_{out}) at the output and is given by:

$$C = \frac{I_{out} \cdot D}{f_s - \Delta V_{out}} \quad (9)$$

Where: I_{out} is the load or charging current, ΔV_{out} is the acceptable output voltage ripple.

C. Modeling and Designing of Lithium-Ion Battery.

In modern power systems, Hybrid Energy Storage Systems (HESS) integrates multiple energy storage devices to enhance overall energy and power performance. Lithium-ion batteries, owing to their high energy density and efficiency, are widely utilized for sustained energy supply in such systems. The incorporation of multiple battery units facilitates improved operational flexibility and effective load management under varying conditions. This configuration enables enhanced load balancing, mitigates stress on individual battery units, and extends overall battery lifespan. Furthermore, it improves system responsiveness and reliability, making it highly suitable for applications such as electric vehicle (EV) charging, renewable energy integration, and microgrid operations.

a. Lithium-Ion Battery Modeling

The lithium-ion battery used in the proposed system is modeled using a nonlinear dynamic equation that captures both charging and discharging characteristics. The battery terminal voltage is expressed as:

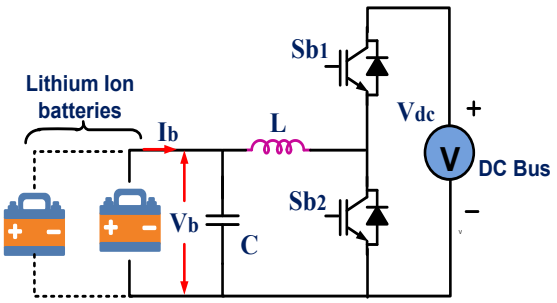

Fig.6 principle operation bidirectional dc-dc buck boost converter

$$E_B = E_0 - \frac{KQI_B}{Q - \int I_B\,dt} - k\frac{Q}{Q - \int I_B\,dt}\int I_B dt + A\exp\left(-B\int I_B\,dt\right) \quad (10)$$

where E_B represents the battery terminal voltage, E_0 is the constant open-circuit voltage, K denotes the polarization constant (V/Ah), Q is the maximum battery capacity (Ah), and IB is the battery current. The term $\int I_B\,dt$) represents the extracted capacity over time. The exponential term $\exp(-B\int I_B\,dt)$ models the voltage behavior in the exponential region of the battery discharge curve, where A and B are empirical constants. This model effectively captures the nonlinear voltage characteristics of lithium-ion batteries under varying load conditions. It accounts for polarization effects, capacity variation, and transient response during charging and discharging. The State of Charge (SoC) of the battery is estimated based on the integration of battery current, enabling accurate monitoring and control of energy storage units. The developed battery model is implemented for each BESS unit in the system, allowing decentralized control and SoC balancing across multiple batteries to enhance system reliability and lifespan.

b. Double-Loop Controller for EV Charging System

A double-loop control system is used as part of the control strategy for electric vehicle (EV) charging in order to guarantee safe, efficient, and reliable charging. The inner current loop controls the current going into the batteries, while the outside voltage loop keeps the DC bus voltage constant. To enhance dynamic performance and decrease steady-state error, a Proportional-Integral (PI) controller is used in both loops.

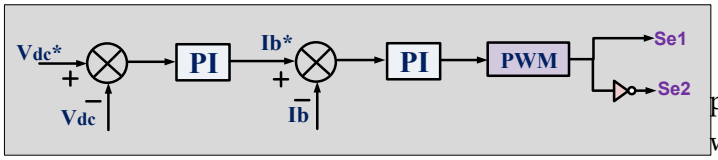

Fig. 7 double loop battery charging controller

1. Outer Voltage Loop: DC Bus Voltage Control

The outer voltage loop ensures the DC bus voltage (V_{dc}) remains stable and within the desired range. Since variations in EV charging loads and grid fluctuations affect the DC bus voltage, this loop provides a reference current (I_{ev}^*) for the inner current loop.

Error Signal Calculation:

$$e_v(t) = V_{dc}^* - V_{dc} \quad (11)$$

PI Controller Output (Reference EV Charging Current I_{ev}^*

$$I_{ev}^*(t) = K_{PV}e_v(t) + k_{iv}\int e_v(t)\,dt \quad (12)$$

Where: I_{ev}^*= Reference charging current for the inner loop, K_{PV} = Proportional gain of voltage controller, k_{iv}= Integral gain of voltage controller

This reference current is then passed to the inner current loop for precise battery charging control.

2. Inner Current Loop: Battery Current Control

To avoid overcharging and battery deterioration, the electric vehicle's inner current loop controls the charging current. Here, the PI controller determines the DC-DC converter's duty cycle, whether it's a buck or a boost.

Error Signal Calculation:

$$e_i(t) = I_{ev}^* - I_{ev} \quad (13)$$

PI Controller Output (Duty Cycle Control)

$$D(t) = K_{Pi}e_i(t) + k_{ii}\int e_i(t)\,dt \quad (14)$$

Where: D = Duty cycle of the DC-DC converter, Kpi= Proportional gain of current controller, Kii= Integral gain of current controller

This duty cycle (D) is applied to the DC-DC converter, adjusting the output voltage and current to regulate battery charging.

D. Wind Power Conversion for EV Charging in DC Microgrid

Multiple power conversion stages are required to provide reliable and efficient power transmission when wind energy is converted in a DC microgrid for the purpose of charging electric vehicles (EVs). After being converted into DC and further adjusted to meet the

microgrid voltage, the variable-frequency AC electricity generated by the wind turbine is delivered to the system. A Permanent Magnet Synchronous Generator (PMSG) is commonly used due to its high efficiency and reliability. The generated AC power is converted into DC using an AC–DC active rectifier, which enables controlled power conversion, improved power quality, and power factor correction. A boost converter is employed to regulate and stabilize the DC output voltage, as wind speed variations lead to fluctuations in generated voltage. Tip Speed Ratio (TSR) control, implemented through Maximum Power Point Tracking (MPPT), allows the Wind Energy Conversion System (WECS) to extract maximum power under varying wind conditions. The regulated DC power is supplied to the microgrid, where it is utilized for EV charging either directly or through Battery Energy Storage Systems (BESS). The BESS mitigates power fluctuations and ensures continuous EV charging by compensating for variations in wind speed and generation. Overall, coordinated operation of the wind turbine, active rectifier, boost converter, and microgrid control system ensures stable voltage regulation and efficient energy distribution, thereby enhancing system reliability and reducing dependence on the utility grid.

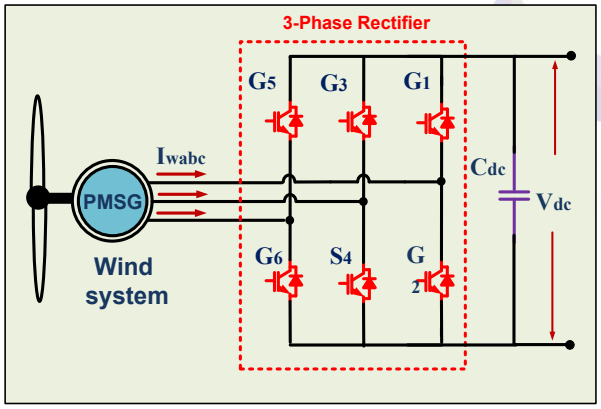

Fig. 8 wind conversion system

1. Wind Power Generation Equation

$$P_\omega = \frac{1}{2}\rho A C_p v_\omega^3 \quad (15)$$

Where: Pw = Wind power output (W), ϱ = Air density (kg/m3), A = Swept area of the turbine (m2), Cp = Power coefficient (typically 0.3 - 0.5), vw = Wind speed (m/s)

2. Tip Speed Ratio (TSR) for MPPT Control

$$\lambda = \frac{\omega R}{v_\omega} \quad (16)$$

Where: λ = Tip speed ratio, ω = Rotor angular velocity (rad/s), R = Blade radius (m)

3. Machine Side Control

The generation of a wind speed reference plays a significant role in the machine side control to extract maximum power from the wind turbine. The control diagram of PMSG connected with active rectifier is shown in Fig. 9. The reference rotor speed is obtained from the optimal tip speed ratio and actual wind speed. The reference speed is:

$$\omega_m^{opt} = \frac{\lambda'_{opt} v_w}{R} \quad (17)$$

where ω_m^{opt} represents reference rotor speed.

The speed error, obtained from the optimal wind speed and actual speed of PMSM, is regulated as reference electromagnetic torque using the PI speed controller, i.e.:

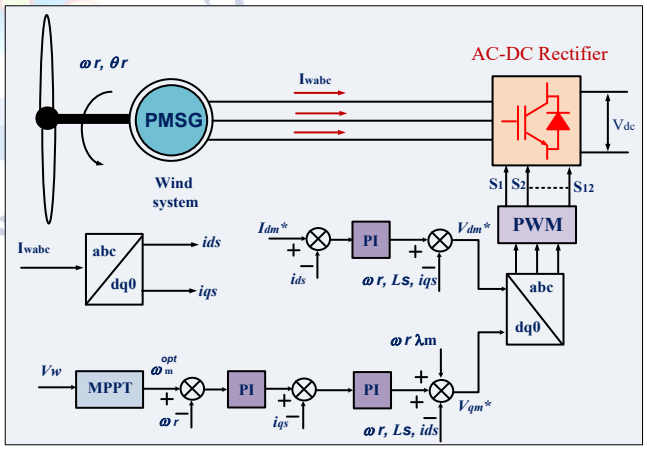

Fig.9 Wind conversion controller

$$\bar{\omega}_r^{error} = \bar{\omega}_m^{opt} - \bar{\omega}_r \quad (18)$$

$$T_e^* = k_{p,s}(\omega_r^{error}) + k_{i,s}\int (\omega_r^{error})\, dt \quad (19)$$

Where $\bar{\omega}_r^{error}$ represents rotor speed error; T_e^* represents reference electromagnetic torque; $k_{p,s}$ represents pro-portional gain of speed controller; and Ki, s represents integral gain of speed controller.

The reference q-axis current is: (i_{qm}^*)

$$i_{qm}^{*} = \frac{4T_e^{*}}{3P} \quad (20)$$

The reference voltage is generated using an inner loop current controller to control the machine side converter. The *d-q* axis references are:

$$v_{dm}^{*} = k_{p,mc}(i_{dm}^{*} - i_{ds}) + k_{i,mc}\int (i_{dm}^{*} - i_{ds})\,dt \; - \omega_e L_s i \quad (21)$$

$$v_{qm}^{*} = k_{p,mc}(i_{qm}^{*} - i_{qs}) + k_{i,mc}\int (i_{qm}^{*} - i_{qs})\,dt - \omega_e(L_s i_{ds} + \lambda_m) \quad (22)$$

where v_{dm}^{*}, v_{qm}^{*} represent reference machine voltage in *d-q* axis; represent reference stator current in *d-q* axis; i_{dm}^{*}, i_{qm}^{*} represents proportional gain of machine current controller; and $k_{p,mc}$, $k_{i,mc}$ represents integral gain of machine current controller. The *d-q* axis machine voltage references are converted into three-phase machine voltage references using inverse park transformation which are fed as in-puts to the pulse width modulation (PWM) generator to generate the switching signal to control the three-phase machine side active rectifier to achieve maximum power from the wind turbine.

Proposed ANN Controller for V_{dc} Voltage Regulation

To enhance the dynamic performance and adaptability of DC-link voltage regulation, an Artificial Neural Network (ANN)-based controller is employed. Unlike conventional controllers, the ANN can effectively handle nonlinearities, uncertainties, and varying operating conditions in hybrid PV–wind–BESS systems.

A. ANN Controller Structure

The ANN used in this work is a feedforward multilayer perceptron (MLP) consisting of an input layer, one hidden layer, and an output layer. The input variables to the ANN are selected as the DC-link voltage error and its rate of change:

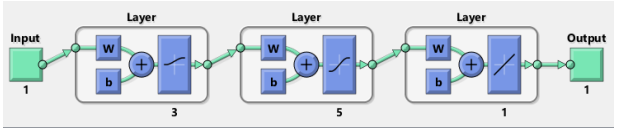

Fig 10: Structure of Neural Network

$$e(k) = V_{dc}^{*} - V_{dc}(k) \quad (23)$$

$$\Delta e(k) = e(k) - e(k-1) \quad (24)$$

where Vdc∗ is the reference DC-link voltage and Vdc(k) is the measured voltage at instant k.

The ANN output u(k) represents the control signal used to regulate the DC-link voltage through power converters.

$$h_j = f\left(\sum_{i=1}^{n} w_{ij}^{(1)} x_i + b_i^{(1)}\right) \quad (25)$$

Where

xi = input variables (e,Δe),

w_{ij} (1) = weights between input and hidden layer,

b_j (1) = bias of hidden neuron,

$f(\cdot)$= activation function (typically sigmoid or ReLU).

The final ANN output is given by:

$$\text{u(k)} = \left(\sum_{j=1}^{n} w_j^{(1)} h_i + b^{(2)}\right) \quad (26)$$

where

$w_j^{(2)}$ = weights from hidden to output layer,

$b^{(2)}$ = output bias.

C. Training of ANN Controller

The ANN is trained using supervised learning to minimize the voltage regulation error. The cost function is defined as:

$$J = \frac{1}{2} e^2\,(\text{k}) \quad (27)$$

The weights are updated using gradient descent (backpropagation):

$$w^{new} = w^{old} - \eta \frac{\partial J}{\partial w} \quad (28)$$

where η is the learning rate.

Training data is generated from system simulations under different operating conditions, including variations in:

- PV irradiance
- Wind speed
- EV load demand
- BESS operating states

D. ANN-Based Control Strategy

The trained ANN generates the control signal u(k), which is used to regulate the DC-link voltage by adjusting the duty cycle of the DC–DC converter or modulation index of the converter. The control objective is to maintain:

$$V_{dc} \approx V_{dc}^{*} \tag{29}$$

under all operating conditions.

IV. RESULTS AND DISCUSSION

A. Performance Analysis of the Proposed Method

Fig. 11 illustrates the power profiles of the PV system, wind generation, and two battery energy storage units (BESS1 and BESS2) under the proposed ANN-based decentralized control strategy. The PV power remains relatively constant at approximately 0.8 kW throughout the operation, indicating stable solar generation. In contrast, the wind power initially operates at a higher level (around 1.8–2 kW) and then experiences a sudden drop to nearly 0.6 kW, representing variability in wind conditions. During the initial period, both BESS1 and BESS2 operate in discharging mode (negative power region), supplying power to support the load demand. The nearly identical discharge profiles of BESS1 and BESS2 demonstrate effective State of Charge (SoC) balancing and equal load sharing between the storage units. As the wind power decreases, the ANN controller adjusts the system operation, causing the batteries to reduce their discharge rate and move toward a balanced operating point. At a later stage, when system conditions change, both BESS units transition to charging mode (positive power region), indicating that excess energy is being stored. This transition occurs smoothly, highlighting the fast dynamic response of the ANN-based decentralized control. The consistent and synchronized behavior of BESS1 and BESS2 confirms proper coordination and uniform utilization of the batteries. Overall, the results clearly demonstrate that the proposed control strategy effectively manages power flow among PV, wind, and multiple BESS units. It ensures stable operation under fluctuating renewable conditions, achieves proper SoC balancing, and enhances system reliability and efficiency.

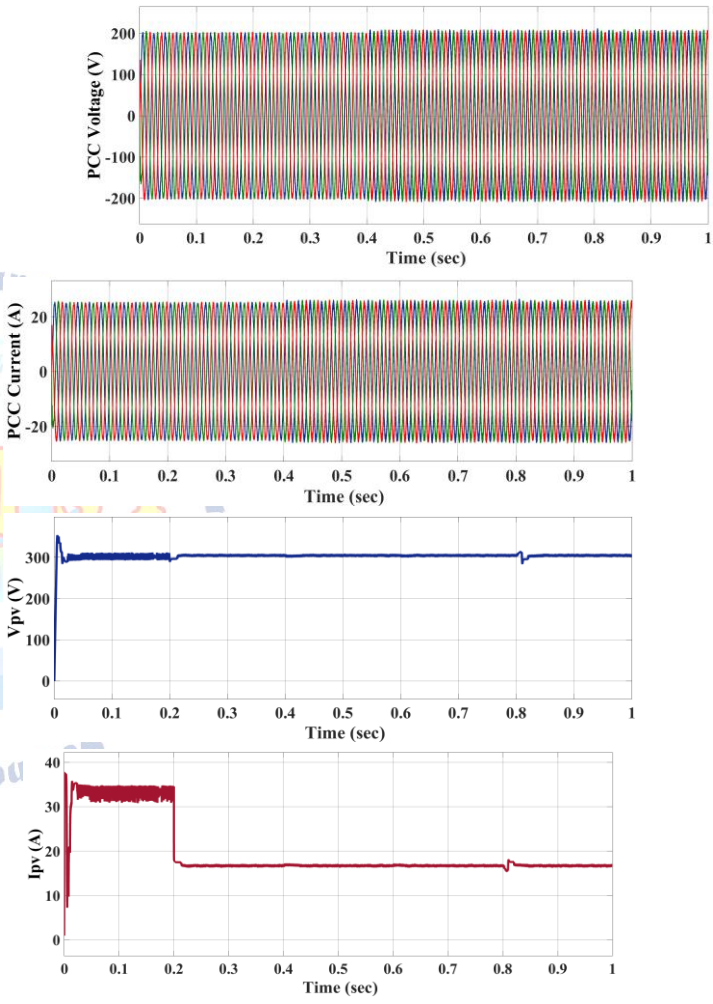

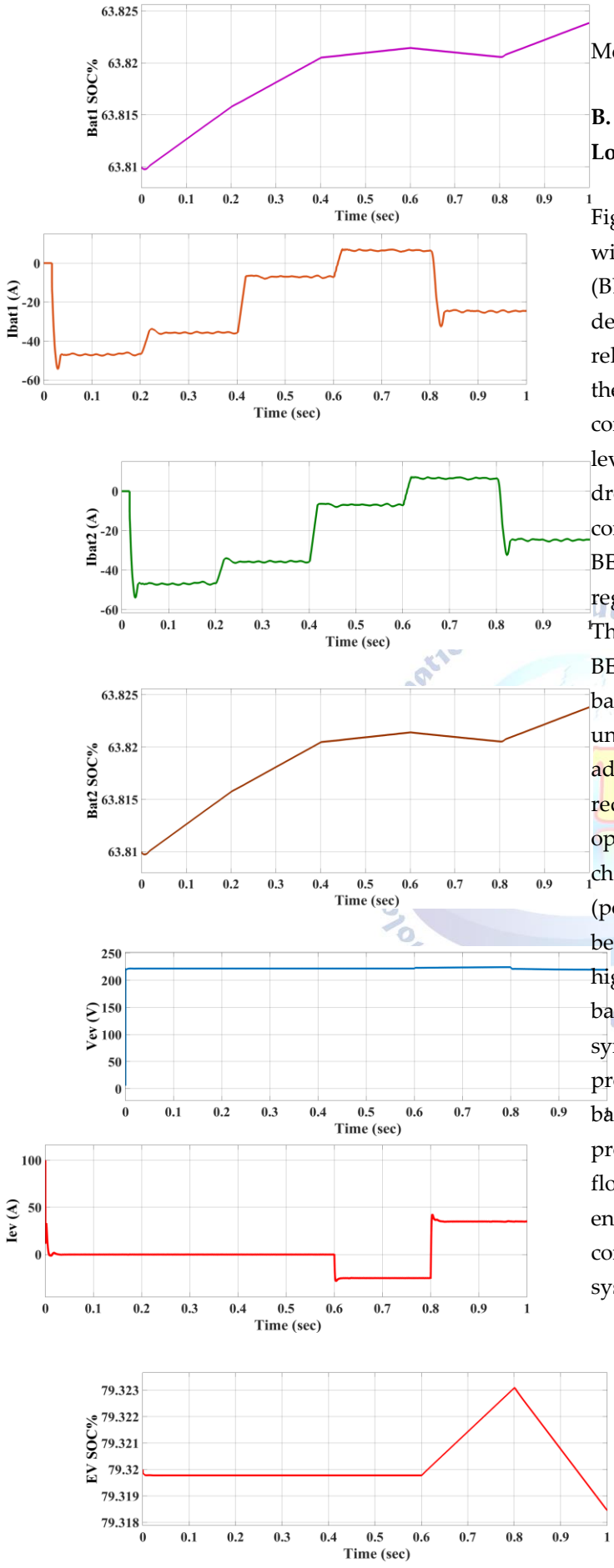

Fig.11 Simulation Results of the Proposed Method Configuration

B. Power Profile Analysis of PV, Wind, BESS, and EV Load

Fig. 12 illustrates the power profiles of the PV system, wind generation, and two battery energy storage units (BESS1 and BESS2) under the proposed ANN-based decentralized control strategy. The PV power remains relatively constant at approximately 0.8 kW throughout the operation, indicating stable solar generation. In contrast, the wind power initially operates at a higher level (around 1.8–2 kW) and then experiences a sudden drop to nearly 0.6 kW, representing variability in wind conditions. During the initial period, both BESS1 and BESS2 operate in discharging mode (negative power region), supplying power to support the load demand. The nearly identical discharge profiles of BESS1 and BESS2 demonstrate effective State of Charge (SoC) balancing and equal load sharing between the storage units. As the wind power decreases, the ANN controller adjusts the system operation, causing the batteries to reduce their discharge rate and move toward a balanced operating point. At a later stage, when system conditions change, both BESS units transition to charging mode (positive power region), indicating that excess energy is being stored. This transition occurs smoothly, highlighting the fast dynamic response of the ANN-based decentralized control. The consistent and synchronized behavior of BESS1 and BESS2 confirms proper coordination and uniform utilization of the batteries. Overall, the results clearly demonstrate that the proposed control strategy effectively manages power flow among PV, wind, and multiple BESS units. It ensures stable operation under fluctuating renewable conditions, achieves proper SoC balancing, and enhances system reliability and efficiency.

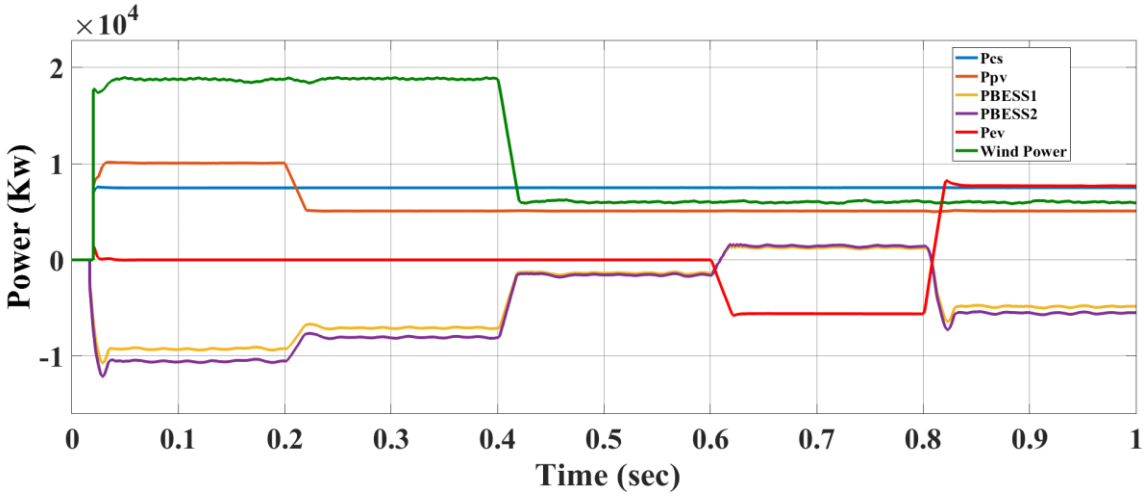

Fig.12 Power Profile Analysis: Simulation Results of the Proposed Method Configuration

VI. CONCLUSION

This paper presented an ANN-based decentralized power management framework for a hybrid PV–wind integrated multi-BESS EV charging infrastructure with State of Charge (SoC) balancing. The proposed approach effectively addressed the challenges associated with the intermittent nature of renewable energy sources and the dynamic behavior of EV charging loads. By employing an Artificial Neural Network (ANN), the system achieved intelligent real-time coordination of power flow among distributed generation sources and multiple battery storage units without relying on a centralized controller. The decentralized control strategy enhanced system scalability, reliability, and resilience, while the implemented SoC balancing mechanism ensured uniform utilization of battery units, thereby reducing degradation and extending battery lifespan. Simulation results demonstrated that the proposed method provides improved voltage stability, efficient power sharing, and faster dynamic response compared to conventional control techniques. Overall, the proposed framework offers a robust and efficient solution for next-generation smart grid applications, particularly in scenarios with high penetration of renewable energy and EV charging demand. Future work may focus on hardware implementation and the integration of advanced learning techniques to further enhance system performance and adaptability.

Conflict of interest statement

Authors declare that they do not have any conflict of interest.

REFERENCES

[1] M. Khalid and B. K. Panigrahi, "SoC-based decentralized power management in multi BESS-PV for EVs charging applications," in Proc. IEEE Glob. Conf. Comput., Power Commun. Technol., 2022, pp. 1–6.

[2] S. Peyghami and F. Blaabjerg, "Power routing: Active asset management in power electronics systems," IEEE Trans. Ind. Appl., vol. 58, no. 5, pp. 6418–6427, Sep./Oct. 2022.

[3] A. Verma, B. Singh, A. Chandra, and K. Al-Haddad, "An implementation of solar PV array based multifunctional EV charger," IEEE Trans. Ind. Appl., vol. 56, no. 4, pp. 4166–4178, Jul./Aug. 2020.

[4] M. Mao et al., "Multi-objective power management for EV fleet with MMC-based integration into smart grid," IEEE Trans. Smart Grid, vol. 10, no. 2, pp. 1428–1439, Mar. 2019.

[5] V. Narayanan, S. Kewat, and B. Singh, "Solar PV-BES based microgrid system with multifunctional VSC," IEEE Trans. Ind. Appl., vol. 56, no. 3, pp. 2957–2967, May/Jun. 2020.

[6] Y. Yang, Q. Ye, L. J. Tung, M. Greenleaf, and H. Li, "Integrated size and energy management design of battery storage to enhance grid integration of large-scale PV power plants," IEEE Trans. Ind. Electron., vol. 65, no. 1, pp. 394–402, Jan. 2018.

[7] S. A. Saleh et al., "On the factors affecting battery unit contributions to fault currents in grid-connected battery storage systems," IEEE Trans. Ind. Appl., vol. 58, no. 3, pp. 3019–3028, May/Jun. 2022.

[8] V. T. Tran, M. R. Islam, K. M. Muttaqi, and D. Sutanto, "An efficient energy management approach for a solar-powered EV battery charging facility to support distribution grids," IEEE Trans. Ind. Appl., vol. 55, no. 6, pp. 6517–6526, Nov./Dec. 2019.

[9] J. Zhou, Y. Xu, H. Sun, Y. Li, and M.-Y. Chow, "Distributed power management for networked AC–DC microgrids with unbalanced microgrids," IEEE Trans. Ind. Inform., vol. 16, no. 3, pp. 1655–1667, Mar. 2020.

[10] S. Kotra and M. K. Mishra, "A supervisory power management system for a hybrid microgrid with HESS," IEEE Trans. Ind. Electron., vol. 64, no. 5, pp. 3640–3649, May 2017.

[11] M. Nabatirad, R. Razzaghi, and B. Bahrani, "Decentralized voltage regulation and energy management of integrated DC microgrids into AC power systems," IEEE J. Emerg. Sel. Topics Power Electron., vol. 9, no. 2, pp. 1269–1279, Apr. 2021.

[12] A. Elmouatamid, R.Ouladsine,M. Bakhouya,N. ElKamoun, M. Khaidar, andK. Zine-Dine, "Reviewof control and energy management approaches in micro-grid systems," Energies, vol. 14, no. 1, Dec. 2020, Art. no. 168.

[13] Z. Ziadi, S. Taira, M. Oshiro, and T. Funabashi, "Optimal power scheduling for smart grids considering controllable loads and high penetration of photovoltaic generation," IEEE Trans. Smart Grid, vol. 5, no. 5, pp. 2350–2359, Sep. 2014.

[14] S. Xie, S. Qi, and K. Lang, "A data-driven power management strategy for plug-in hybrid electric vehicles including optimal battery depth of discharging," IEEE Trans. Ind. Inform., vol. 16, no. 5, pp. 3387–3396, May 2020.

[15] M. Hosseinzadeh and F. R. Salmasi, "Fault-tolerant supervisory controller for a hybrid AC/DC micro-grid," IEEE Trans. Smart Grid, vol. 9, no. 4, pp. 2809–2823, Jul. 2018.

[16] J. M. Raya-Armenta et al., "Energy management system optimization in islanded microgrids: An overview and future trends," Renewable Sustain. Energy Rev., vol. 149, pp. 1364–0321, Oct. 2021.

[17] T. Dragiˇcevi´c, S. Suˇci´c, J. C. Vasquez, and J. M. Guerrero, "Flywheelbased distributed bus signalling strategy for the public fast charging station," IEEE Trans. Smart Grid, vol. 5, no. 6, pp. 2825–2835, Nov. 2014.

[18] A. Kirakosyan, E. F. El-Saadany, M. S. E. Moursi, A. H. Yazdavar, and A. Al-Durra, "Communication-free current sharing control strategy for DC microgrids and its application forAC/DC hybrid microgrids," IEEE Trans. Power Syst., vol. 35, no. 1, pp. 140–151, Jan. 2020.

[19] J.-H. Teng, S.-H. Liao, and C.-K. Wen, "Design of a fully decentralized controlled electric vehicle charger for mitigating charging impact on power grids," IEEE Trans. Ind. Appl., vol. 53, no. 2, pp. 1497–1505, Mar./Apr. 2017.

[20] G. Liu, T. Caldognetto, P.Mattavelli, and P.Magnone, "Power-based droop control in DC microgrids enabling seamless disconnection from upstream grids," IEEE Trans. Power Electron., vol. 34, no. 3, pp. 2039–2051, Mar. 2019.

International Journal for Modern Trends in Science and Technology